Improving the theoretical prediction for the $B_s - \bar{B}_s$ width difference: matrix elements of next-to-leading order $\Delta B = 2$ operators

Christine Davies[1], *Judd* Harrison[2], *G Peter* Lepage[3], *Christopher* Monahan[4,5], *Junko* Shigemitsu[6], and *Matthew* Wingate[2,⋆]

[1] *SUPA, School of Physics and Astronomy, University of Glasgow, Glasgow G12 8QQ, United Kingdom*
[2] *DAMTP, University of Cambridge, Cambridge CB3 0WA, United Kingdom*
[3] *Laboratory of Elementary Particle Physics, Cornell University, Ithaca, NY 14853, United States*
[4] *New High Energy Theory Center and Department of Physics and Astronomy, Rutgers, the State University of New Jersey, Piscataway, NJ 08854, United States*
[5] *Institute for Nuclear Theory, University of Washington, Seattle, WA 98195-1550, United States*
[6] *Department of Physics, Ohio State University, Columbus, Ohio 43210, United States*

Abstract. We present lattice QCD results for the matrix elements of R_2 and other dimension-7, $\Delta B = 2$ operators relevant for calculations of $\Delta\Gamma_s$, the $B_s - \bar{B}_s$ width difference. We have computed correlation functions using 5 ensembles of the MILC Collaboration's 2+1+1-flavour gauge field configurations, spanning 3 lattice spacings and light sea quarks masses down to the physical point. The HISQ action is used for the valence strange quarks, and the NRQCD action is used for the bottom quarks. Once our analysis is complete, the theoretical uncertainty in the Standard Model prediction for $\Delta\Gamma_s$ will be substantially reduced.

1 Introduction

Mixing between particle and antiparticle states of neutral mesons has now been observed in K^0, D^0, B^0, and B_s^0 mesons. These mixings are due to couplings between generations of quark $SU(2)_L$ doublets after electroweak symmetry breaking. Since the leading-order weak process, represented by the "box" diagrams, is at 1-loop level, there is the chance that new heavy particles, beyond those in the Standard Model, could cause differences between Standard Model predictions and experimental results.

To a good approximation, three parameters are sufficient to describe neutral meson mixing: the moduli of the off-diagonal matrix elements of the 2×2 mass and width matrices, M and Γ, and their relative phase $\phi = \arg(-M_{12}/\Gamma_{12})$. For the B_s^0 system these parameters are constrained by experimental measurements of the B_s^0-$\bar{B}_s^0$ mass difference, width difference, and a flavour-specific CP asymmetry:

$$\Delta M_s = 2|M_{12}^s|\,, \quad \Delta\Gamma_s = 2|\Gamma_{12}^s|\cos\phi_s\,, \text{ and } a_{\rm fs}^s = \frac{\Delta\Gamma_s}{\Delta M_s}\tan\phi_s\,. \tag{1}$$

In (1) and the remainder of this paper we use notation specific to B_s^0 mixing. See Ref. [1] for a recent review of B_s^0 mixing and references to a rich literature.

⋆ Speaker, e-mail: M.Wingate@damtp.cam.ac.uk

The calculation of $\Delta\Gamma_s$ within the Standard Model is summarized in Ref. [2]. Contributions to Γ_{12}^s come from matrix elements of the non-local product of 2 $\Delta B = 1$ effective Hamiltonians

$$\mathscr{T} = \mathrm{Im}\, i \int d^4x\, \mathcal{T}\, H_{\mathrm{eff}}^{\Delta B=1}(x)\, H_{\mathrm{eff}}^{\Delta B=1}(0)\,. \tag{2}$$

The contributions from charm and up quarks in the intermediate states depend on the corresponding CKM matrix elements; i.e. $\Gamma_{12}^s = -(\lambda_c^2\Gamma_{12}^{cc} + 2\lambda_c\lambda_u\Gamma_{12}^{uc} + \lambda_u^2\Gamma_{12}^{uu})$ with $\lambda_i = V_{is}^* V_{ib}$. At the present level of accuracy, only the CKM-leading contribution from Γ_{12}^{cc} is important.

Direct lattice QCD calculation of matrix elements such as $\langle \bar{B}_s|\mathscr{T}|B_s\rangle$ is not generally feasible due to the difficulty in correctly treating all intermediate states.[1] However, one can employ an operator product expansion known as the heavy quark expansion (HQE). Order-by-order in Λ_{QCD}/m_B, one relates the matrix elements of nonlocal operators to a series of matrix elements of local $\Delta B = 2$ operators. Using the most advantageous basis [2] the charm-charm loop contribution to Γ_{12}^s is given by

$$\Gamma_{12}^{cc} = \frac{G_F^2 m_b^2}{24\pi m_{B_s}}\left[\left(G + \frac{\alpha_2}{2}G_S\right)\langle \bar{B}_s|Q_1|B_s\rangle + \alpha_1 G_S\langle \bar{B}_s|Q_3|B_s\rangle\right] \;+\; \tilde{\Gamma}_{12,1/m_b}^{cc}\,, \tag{3}$$

with the next order in the HQE given by

$$\tilde{\Gamma}_{12,1/m_b}^{cc} = \frac{G_F^2 m_b^2}{24\pi m_{B_s}}\left\{g_0^{cc}\langle \bar{B}_s|R_0|B_s\rangle + \sum_{j=1}^{3}\left[g_j^{cc}\langle \bar{B}_s|R_j|B_s\rangle + \tilde{g}_j^{cc}\langle \bar{B}_s|\tilde{R}_j|B_s\rangle\right]\right\}. \tag{4}$$

A full basis of dimension-6 $\Delta B = 2$ operators can be written as

$$\begin{aligned}
Q_1 &= (\bar{b}^\alpha\gamma^\mu(1-\gamma^5)s^\alpha)(\bar{b}^\beta\gamma_\mu(1-\gamma^5)s^\beta)\,, & Q_4 &= (\bar{b}^\alpha(1-\gamma^5)s^\alpha)(\bar{b}^\beta(1+\gamma^5)s^\beta)\\
Q_2 &= (\bar{b}^\alpha(1-\gamma^5)s^\alpha)(\bar{b}^\beta(1-\gamma^5)s^\beta)\,, & Q_5 &= (\bar{b}^\alpha(1-\gamma^5)s^\beta)(\bar{b}^\beta(1+\gamma^5)s^\alpha)\\
Q_3 &= (\bar{b}^\alpha(1-\gamma^5)s^\beta)(\bar{b}^\beta(1-\gamma^5)s^\alpha)\,.
\end{aligned} \tag{5}$$

At higher order in the HQE, one needs matrix elements of the following operators

$$\begin{aligned}
R_0 &= Q_2 + \alpha_1 Q_3 + \frac{1}{2}\alpha_2 Q_1\\
R_1 &= \frac{m_s}{m_b}(\bar{b}^\alpha(1-\gamma^5)s^\alpha)(\bar{b}^\beta(1+\gamma^5)s^\beta) = \frac{m_s}{m_b}Q_4\\
R_2 &= \frac{1}{m_b^2}(\bar{b}^\alpha\overleftarrow{D}_\rho\gamma^\mu(1-\gamma^5)D^\rho s^\alpha)(\bar{b}^\beta\gamma_\mu(1-\gamma^5)s^\beta)\\
R_3 &= \frac{1}{m_b^2}(\bar{b}^\alpha\overleftarrow{D}_\rho(1-\gamma^5)D^\rho s^\alpha)(\bar{b}^\beta(1-\gamma^5)s^\beta)\,.
\end{aligned} \tag{6}$$

Matrix elements of the Q_i operators (5) have long been calculated using lattice QCD; unquenched results for B_s mixing appear in [4–7]. Until this work there have been no calculations of R_2 and R_3 matrix elements. In phenomenological analyses [2, 8] the vacuum saturation approximation was used, allowing a 50% uncertainty. Sum rule estimates suggest these matrix elements should be within a few percent of the vacuum saturation approximation values [9], although the VSA predictions depend sensitively on the value of the b-quark pole mass.

Table 1. Parameters of the ensembles used in this calculation.

label	a/fm	$am_\ell^{\rm sea}$	$am_s^{\rm sea}$	$am_c^{\rm sea}$	$N_s^3 \times N_t$	$am_s^{\rm val}$	am_b
VC5	0.1474(5)(14)(2)	0.013	0.0650	0.838	$16^3 \times 48$	0.0641	3.297
VCp	0.1450(3)(14)(2)	0.00235	0.0647	0.831	$32^3 \times 48$	0.0628	3.25
C5	0.1219(2)(9)(2)	0.0102	0.0509	0.635	$24^3 \times 64$	0.0522	2.66
Cp	0.1189(2)(9)(2)	0.00184	0.0507	0.628	$48^3 \times 64$	0.0507	2.62
F5	0.0873(2)(5)(1)	0.0074	0.037	0.440	$32^3 \times 96$	0.0364	1.91

2 Method

We use MILC's HISQ ensembles, which include sea quark effects of degenerate up and down quarks and physical-mass strange and charm quarks [10, 11]. We use the HISQ action for the valence s quark and the NRQCD action for the b quark. The 5 ensembles include 3 distinct lattice spacings which we respectively refer to as fine (F), coarse (C), and very coarse (VC). For each of these spacings we use configurations with dynamical pion mass of approximately 300 MeV, and for the coarse and very coarse spacings, we used the physical ensembles which have pion mass approximately 130 MeV. Table 1 lists specific input parameters and the lattice spacings as determined from the $\Upsilon(2S-1S)$ splitting [12, 13].

In carrying out the calculation of $\langle \bar{B}_s|R_i|B_s\rangle$, with $i = 2, 3$, we need not compute all 4 terms in the Lorentz dot product (6). The temporal derivative acting on the b field is $O(m_b)$: $\bar{b}\overleftarrow{D}_0 = \pm m_b \bar{b}\gamma_0$, the sign depending on whether we have an outgoing b quark or incoming $\bar{b}$ antiquark. Thus we can write

$$\frac{1}{m_b^2}(\bar{b}^\alpha \overleftarrow{D}_\rho \Gamma D^\rho s^\alpha) = \frac{1}{m_b^2}(\bar{b}^\alpha \overleftarrow{D}_0 \Gamma D^0 s^\alpha) + O\left(\frac{1}{m_b^2}\right). \tag{7}$$

Applying the equations of motion, $i\gamma_0 D^0 s = (\vec{\gamma}\cdot\vec{D})s$, we arrive at

$$R_{2,3} = \pm\frac{1}{m_b}(\bar{b}^\alpha \Gamma\gamma_0(\vec{\gamma}\cdot\vec{D})s^\alpha)(\bar{b}^\beta\Gamma s^\beta)\,. \tag{8}$$

The lattice calculation of $\langle \bar{B}_s|R_{2,3}|B_s\rangle$ proceeds just as for the Q_j matrix elements, except for the need to have a derivative operate on the strange quark at the operator. In addition to needing a staggered propagator $g(y,z)$ computed from local source [14]

$$K(x,y)\,g(y,z) = \delta(x,z)\,, \tag{9}$$

we need propagators from a point-split source ($k = 1, 2, 3$)

$$K(x,y)\,g^{(k)}(y,z) = \frac{1}{2}\left[\delta(x,z+\hat{k}a)U_k^\dagger(z) - \delta(x,z-\hat{k}a)U_k(z-\hat{k}a)\right]. \tag{10}$$

Naive quark propagators are constructed from staggered propagators via

$$\begin{aligned} G(y,z) &= \Omega(y)\,g(y,z)\,\Omega^\dagger(z) \\ G^{(k)}(y,z) &= \Omega(y)\,g^{(k)}(y,z)\,\Omega^\dagger(z\pm\hat{k}a) \end{aligned} \tag{11}$$

where $\Omega(x) = \prod_{\mu=0}^{3}(\gamma_\mu)^{x_\mu/a}$. Since we will need to sum over spatial directions, we require 4 strange quark inversions on each configuration and for each source location.

[1] Progress is being made in the kaon system with heavier than physical quark masses, where the only intermediate state with energy less than m_K is the π^0 [3].

Table 2. Perturbative subtraction coefficients used in (14), for the values of am_b used on each ensemble.

Coefficient	VC5	VCp	C5	Cp	F5
ξ_{21}	−0.1311	−0.1327	−0.1557	−0.1573	−0.2004
ξ_{22}	0.0092	0.0093	0.013	0.0133	0.0225
ξ_{31}	−0.0331	−0.0334	−0.0392	−0.0397	−0.0508
ξ_{32}	−0.2829	−0.2864	−0.3404	−0.3449	−0.451

3 Perturbative matching

One-loop matching between the lattice theory and the continuum $\overline{\text{MS}}$ renormalization schemes has been carried out for the Q_i operators, including tree-level $1/m_b$ corrections [15]. The 1-loop mixing between operators is parametrized by the ρ_{ij} matrix and $1/m_b$ corrections are given by $\hat{Q}^{\text{sub}}_{i,1}$, which are of the form $\frac{1}{2m_b}(D_k\bar{b}^\alpha\gamma^k\Gamma_1 s^\alpha)(\bar{b}^\beta\Gamma_2 s^\beta)$:

$$Q_i^{\overline{\text{MS}}} = \hat{Q}_i + \alpha_s\rho_{ij}\hat{Q}_j + \hat{Q}^{\text{sub}}_{i,1}\,. \tag{12}$$

Because derivatives are implemented as finite difference operators the $\frac{1}{a}\hat{Q}_i$ mix with $\hat{Q}_{i,1}$; this can similarly be computed in perturbation theory. We define a subtracted operator which gives a more accurate determination of the next-to-leading contribution:

$$\hat{Q}^{\text{sub}}_{i,1} = \hat{Q}_{i,1} - \alpha_s\zeta_{ij}\hat{Q}_j\,. \tag{13}$$

The coefficients ρ_{ij} and ζ_{ij} are tabulated in [15].

A similar subtraction is done here for the $R_{2,3}$ operators:

$$\hat{R}^{\text{sub}}_i = \hat{R}_i - \alpha_s\xi_{ij}\hat{Q}_j\,. \tag{14}$$

Values for ξ_{ij} are given in Table 2. We use the α_V values as tabulated in [16]. Note that we have not carried out the 1-loop matching between lattice and $\overline{\text{MS}}$ schemes for $\hat{Q}^{\text{sub}}_{i,1}$ or $\hat{R}^{\text{sub}}_i$. Therefore our results for their $\overline{\text{MS}}$ matrix elements will have an $O(\alpha_s)$ systematic uncertainty.

4 Fits to correlation functions

On each of the 1000 or so configurations in the 5 ensembles listed in Table 1, we created strange quark propagators with inversion sources on 2 timeslices per configuration – except for the VC5 ensemble where we weighed the benefits of doubling the number of sources per configuration.[2] We calculated 3-point functions with local B_s and $\bar{B}_s$ sinks as well as Gaussian smeared sinks with 2 radii. The smearing was done with the links fixed to Coulomb gauge. The 2-point correlators are taken from earlier work where 16 sources per configuration were used [13].

Correlator data are fit to functions of the form

$$C^{\text{2pt}}_{ab}(t) = \sum_i X_{a,i}X_{b,i}e^{-E_i t} + \sum_i (-1)^{t/a}Y_{a,i}Y_{b,i}e^{-E^o_i t} \tag{15}$$

$$\tag{16}$$

[2] We concluded that increased statistics were not sufficiently beneficial to warrant the cost of doubling the data set on other ensembles.

Table 3. Ranges in Euclidean time used for fits to correlation functions. Numbers are given in lattice units.

Ensemble(s)	$t_{\rm min}$	$t^{\rm 2pt}_{\rm max}$	T
VC5, VCp	5	17	11, 12, 13
C5, Cp	6	21	13, 14, 15, 16
F5	9	40	19, 20, 21, 22, 23, 24, 25

and

$$C^{\rm 3pt}_{ab}(t,T) = \sum_{i,j} X_{a,i} V_{nn,ij} X_{b,j} e^{-E_i t} e^{-E_j (T-t)} \; + \; \text{oscillating} \tag{17}$$

using the `corrfitter` package [17]. The oscillating states in (16) and (17) appear due to opposite-parity temporal doublers present in staggered quark formulations. In (17), t is the temporal distance between the initial state interpolating operator and the 4-quark operator and T is the distance between the initial and final state interpolating operators. Values used in the fits presented here are given in Table 3.

The Gaussian priors for the fit amplitudes and energies were set as follows. We first performed 2-exponential fits ($N = 2$ exponentials in each parity channel) to the 2-point data using wide priors and $t_{\rm min} \gtrsim 1.2$ fm. From the output of this fit we took the ground state energy and amplitude, multiplied their uncertainties by 10, and used this as the prior means and half-widths for subsequent fits. For the excited states, we took the energy splittings to be $O(a\Lambda_{\rm QCD}) \pm 50\%$ and the amplitudes to be 0 ± 1.

After fixing the priors for the energies and 2-point amplitudes, we performed $N = 3$ fits to 3-point correlator data with $t_{\rm min} \approx 1.0$ fm and 2 large values of T using 0 ± 1 for the priors on the V fit parameters. This gave an order-of-magnitude estimate for the ground state amplitude. In subsequent fits we set the prior on $V_{nn,00}$ to be the fit result $\pm 50 - 100\%$; for the amplitudes in the oscillating terms, we used standard deviations of $100 - 400\%$ of the results from the preliminary fits.

In the fits presented below, we found that convergence was improved by first fitting the 2-point correlator data and using the results as priors for the fits to the 3-point correlators. In most cases the difference between these "chained" fits and fully simultaneous fits is not significant [18]; however, there were some cases where the simultaneous fits failed to converge.

In Fig. 1 we show preliminary results of fits to the 3-point amplitudes $V_{nn,00}$ determining the R_2 and R_3 matrix elements. We observe results which give consistent results once enough exponentials are included to account for excited state contributions to the correlators. In order to obtain this, it was necessary to impose an SVD cut of 0.001 on the correlation matrix whose smaller singular values are not well-determined by the data.

Figure 2 shows preliminary results vs. a^2 for matrix elements of R_2 and R_3 after subtraction (14), on the VC5, C5, and F5 ensembles. The fits on the physical point ensembles VCp and Cp are not as far along in the process of being checked. We are still assessing fitting uncertainties and ensuring results are robust against different fitting choices. What we present here are the results of separate fits to correlators for the operators R_2, R_3, Q_1, and Q_2. Once we have finished investigating these fits, we will form the linear combinations of correlators, configuration-by-configuration, which will allow us to determine matrix elements of $R_2^{\rm sub}$ and $R_3^{\rm sub}$ directly.

5 Outlook

We presented preliminary results for $\langle \bar{B}_s | R_2 | B_s \rangle$ and $\langle \bar{B}_s | R_3 | B_s \rangle$ on 5 ensembles spanning a range of 3 lattice spacing and including 2 physical mass ensembles. We are presently verifying stability of fit

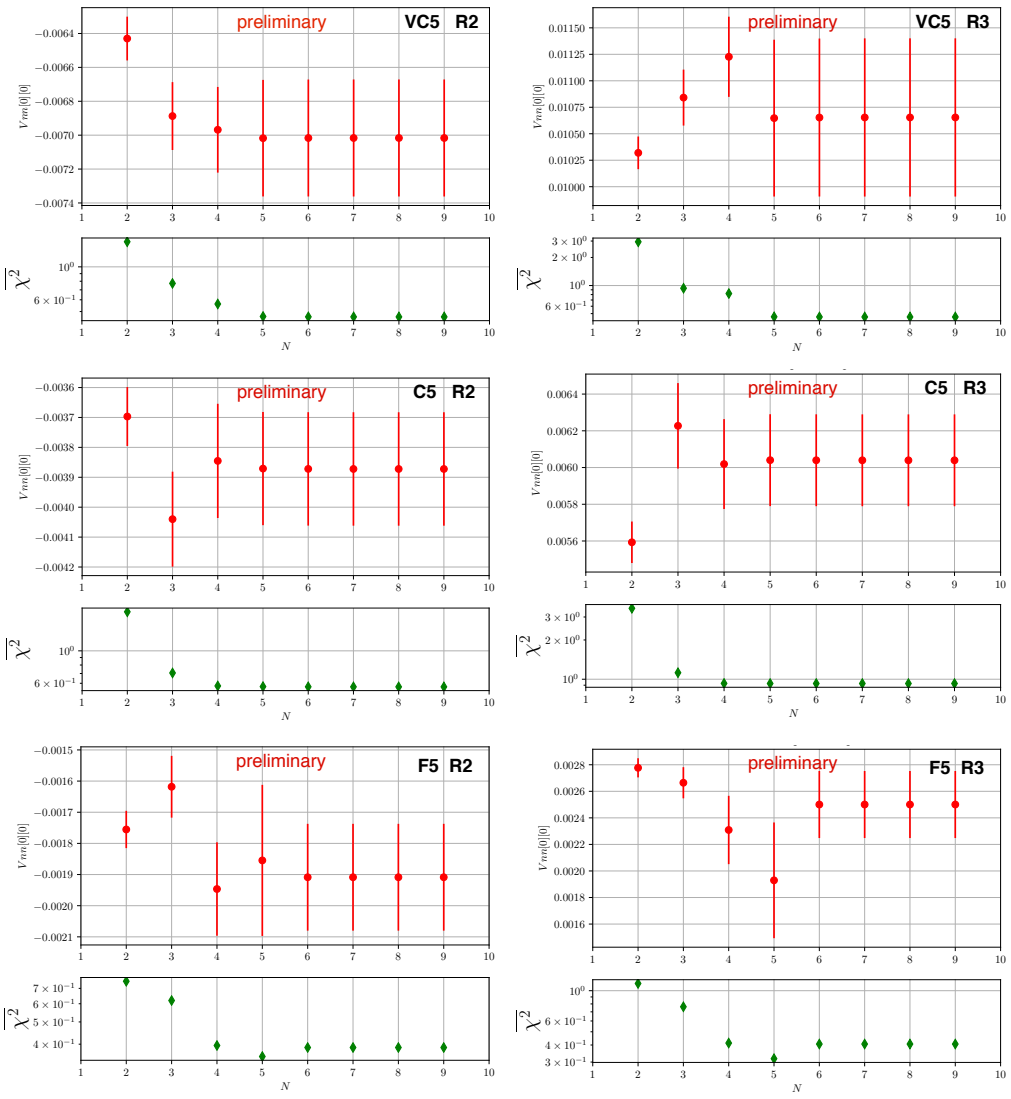

Figure 1. Fit results (upper plots) and χ^2 per degree-of-freedom (lower plots) for unsubtracted R_2 and R_3 fit amplitudes ($V_{nn,00}$) for increasing number of exponentials (Eq. 17) on the VC5, C5, and F5 ensembles. N is equal to the number of energies in the nonoscillating channel (desired parity) and the number of energies in the oscillating channel.

results. The statistical precision may be improved by performing fits to the linear combinations of correlators directly yielding the 1-loop subtracted matrix elements. The results from different ensembles will then enable an assessment of discretization and quark-mass tuning effects. We expect the dominant uncertainty to be due to the $O(\alpha_s)$ difference between lattice and continuum regularization schemes. This will be the first time these matrix elements have been computed using lattice QCD.

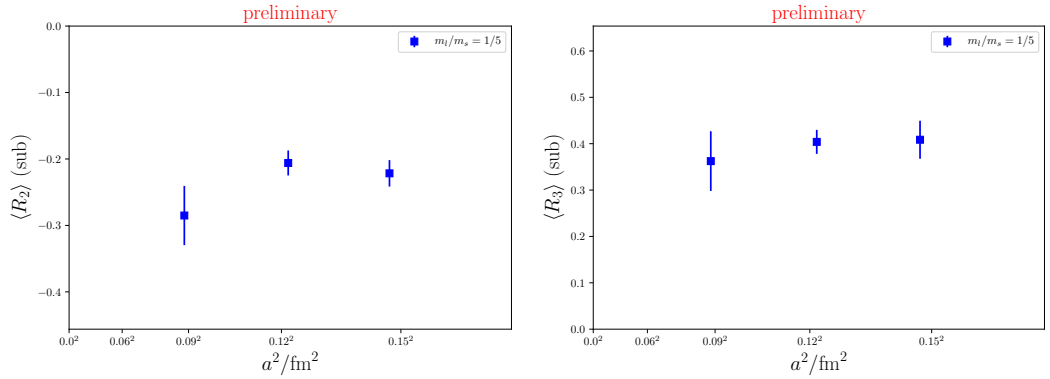

Figure 2. Results (in GeV^4) for subtracted R_2 and R_3 matrix elements on the ensembles with $m_\ell/m_s = 1/5$. Error bars shown only include statistical and fitting uncertainties. The vacuum saturation approximation gives $\langle R_2 \rangle^{\mathrm{VSA}} = -0.3\ \mathrm{GeV}^4$ and $\langle R_3 \rangle^{\mathrm{VSA}} = 0.5\ \mathrm{GeV}^4$.

Acknowledgments

We thank the MILC collaboration for their gauge configurations and their code MILC-7.7.11 [19]. This work was funded in part by STFC grants ST/L000385/1 and ST/L000466/1. CJM is supported in part by the US Department of Energy through Grant Number DE-FG02-00ER41132. Results described here were obtained using the Darwin Supercomputer of the University of Cambridge High Performance Computing Service as part of the DiRAC facility jointly funded by STFC, the Large Facilities Capital Fund of BIS and the Universities of Cambridge and Glasgow. This equipment was funded by BIS National E-infrastructure capital grant (ST/K001590/1), STFC capital grants ST/H008861/1 and ST/H00887X/1, and STFC DiRAC Operations grants ST/K00333X/1, ST/M007073/1, and ST/P002315/1. MW is grateful for an IPPP Associateship held while this work was undertaken and for discussions with A Lenz.

References

[1] M. Artuso, G. Borissov, A. Lenz, Rev. Mod. Phys. **88**, 045002 (2016), 1511.09466

[2] A. Lenz, U. Nierste, J. High Energy Phys. **06**, 072 (2007), hep-ph/0612167

[3] Z. Bai, N.H. Christ, T. Izubuchi, C.T. Sachrajda, A. Soni, J. Yu, Phys. Rev. Lett. **113**, 112003 (2014), 1406.0916

[4] E. Gamiz et al. (HPQCD), Phys. Rev. D **80**, 014503 (2009), 0902.1815

[5] N. Carrasco et al. (ETM), JHEP **03**, 016 (2014), 1308.1851

[6] R. Dowdall, C. Davies, R. Horgan, G.P. Lepage, C. Monahan, J. Shigemitsu, PoS **LATTICE2014**, 373 (2014), 1411.6989

[7] A. Bazavov et al. (Fermilab Lattice, MILC), Phys. Rev. D **93**, 113016 (2016), 1602.03560

[8] T. Jubb, M. Kirk, A. Lenz, G. Tetlalmatzi-Xolocotzi, Nucl. Phys. **B915**, 431 (2017), 1603.07770

[9] T. Mannel, B.D. Pecjak, A.A. Pivovarov (2007), hep-ph/0703244

[10] A. Bazavov et al. (MILC), Phys. Rev. D **82**, 074501 (2010), 1004.0342

[11] A. Bazavov et al. (MILC), Phys. Rev. D **87**, 054505 (2013), 1212.4768

[12] R. Dowdall et al., Phys. Rev. D **85**, 054509 (2012), 1110.6887

[13] R.J. Dowdall, C.T.H. Davies, R.R. Horgan, C.J. Monahan, J. Shigemitsu, Phys. Rev. Lett. **110**, 222003 (2013), 1302.2644

[14] M. Wingate, J. Shigemitsu, C.T.H. Davies, G.P. Lepage, H.D. Trottier, Phys. Rev. D **67**, 054505 (2003), hep-lat/0211014

[15] C. Monahan, E. Gamiz, R. Horgan, J. Shigemitsu, Phys. Rev. D **90**, 054015 (2014), 1407.4040

[16] B. Colquhoun, C.T.H. Davies, R.J. Dowdall, J. Kettle, J. Koponen, G.P. Lepage, A.T. Lytle, Phys. Rev. D **91**, 114509 (2015), 1503.05762

[17] G.P. Lepage, github.com/gplepage/corrfitter.git

[18] C.M. Bouchard, G.P. Lepage, C. Monahan, H. Na, J. Shigemitsu, Phys. Rev. D **90**, 054506 (2014), 1406.2279

[19] MILC Code Repository, https://github.com/milc-qcd